CFD Letters

Journal homepage:
https://semarakilmu.com.my/journals/index.php/CFD_Letters/index
ISSN: 2180-1363

Feasibility Study of Small-Diameter Pico-Hydro Breastshot Waterwheel by Computational Method

Dewi Puspita Sari[1], Dendy Adanta[1,2,*], Imam Syofii[1], Wadirin[1], Aji Putro Prakoso[3], Dadan Hermawan[3], Ahmed Al-Manea[4], Ramiz Ibraheem Saeed[5], Ahmad Fudholi[2,6], Subagyo[2]

[1] Study Program of Mechanical Engineering, Faculty of Teacher Training and Education, Universitas Sriwijaya, Ogan Ilir – 30662, Indonesia
[2] Research Center for Energy Conversion and Conservation, National Research and Innovation Agency (BRIN), Serpong, 15314, Indonesia
[3] Department of Mechanical Engineering, Universitas Jenderal Achmad Yani (UNJANI), Cimahi – Bandung, Indonesia
[4] Samawa Technical Institute, Al-Furat Al-Awsat Technical University, Iraq
[5] Department of Mechanical Engineering, Faculty of Engineering, University of Mosul, Mosul, Iraq
[6] Solar Energy Research Institute, Universiti Kebangsaan Malaysia, 43600 Bangi, Selangor, Malaysia

ARTICLE INFO

Article history:
Received 27 May 2023
Received in revised form 23 June 2023
Accepted 24 July 2023
Available online 1 November 2023

Keywords:
Pico-Hydro; Waterwheel; Breastshot; Computational Method

ABSTRACT

Breastshot water wheels have very good simplicity, efficiency, and low head working range which is suitable for use in tropical rainforest villages in Indonesia. One of the weaknesses of the breastshot water wheel is that it has a very slow rotational speed which makes it need a high transmission ratio to be coupled with the generator. This study investigates the performance of a breastshot water wheel at smaller diameters and modifying the bucket inlet angle (36°, 49°, 71°, and 90°) by the computational fluid dynamics (CFD) method. In this case, the breastshot waterwheel's diameter ratio is equal to the head. Based on CFD results, the new configuration (this study) allowed us to increase the rotational speed to 30 to 35 rpm, higher than typical rotational speeds of breastshot water wheels of less than 10 rpm. Then, the bucket inlet angle and wheel rotation affect the performance of the breastshot waterwheel and are expressed using empirical law. Based on the empirical law approach, the 49° bucket is recommended because it has a stable efficiency above 60% and a wide operating range; the large discharge fluctuations do not change the turbine performance significantly.

1. Introduction

Off-grid electricity development can help accelerate isolated rural areas [1]. Waterwheels have been used to transform the potential energy from water streams into usable energy for hundreds of years [2]. As the traditional hydropower machine, breastshot waterwheels have good simplicity, efficiency, and low head working range [3,4], thus are suitable to be used in tropical rainforest villages in Indonesia [5]. However, there is still a lack of study about this water wheel to improve its ability to produce electricity, especially on the power take off-grid system [6,7].

There are several studies focused on breastshot water wheels. Muller *et al.,* [8] developed a procedure to design a breastshot water wheel with an overflow inlet. The procedure considers the

* *Corresponding author.*
E-mail address: dendyadanta@ymail.com (Dendy Adanta)

https://doi.org/10.37934/cfdl.15.11.169180

water transfer at the inlet, the downstream energy transfer, and the water outflow. This paper also mentions some recommendations from a previous study [9], where the water wheel diameter (D) was suggested to be equal to the potential head (H) added 3.5 m (D=H+3.5 m) or about twice the H. The laboratory-scaled experiment testing reported the maximum waterwheel efficiency was about 87% at the wheel tangential velocity and water absolute velocity ratio (U/C_1) of 0.6 [8]. More suggestions about D are reported in Quaranta and Revelli [16].

Quaranta and Revelli conducted several studies about breastshot wheels during 2015-2018. The first study developed an analytical approach for estimating power losses inside a breastshot water wheel, validated using experimental testing [10]. To design a breastshot waterwheel, some losses should be considered: hydraulically losses, impact losses, and leakage losses, which should be minimized, especially by optimizing the inflow [10]. Another study was conducted to find the optimal filling ratio by varying the water inflow: the optimal filling ratio was about 50% [11]. Another Quaranta and Revelli study was the search for the optimum bucket number for breastshot wheels, finding that it is 48 for the investigated wheel. Still, a general rule was also proposed to generalize results [12]. Another study about bucket number has conducted by Warjito *et al.,* [13], concluding that the breastshot water wheel bucket number impacts its performance, affecting the exchange of kinetic and hydrostatic energy, as confirmed in [12]. However, the increment of kinetic energy in water inflow does not increase or decrease this waterwheel's performance [14,15]; it means this waterwheel could self-adjust the water inflow energy. Besides that, incrementing inlet velocity, for example, by increasing the channel angle slope, can increase the rotational speed [14,15].

One weakness of the breastshot waterwheel is its very slow rotational speed (n) [15]. All these studies discussed shown the optimum n is between 7.5 to 20 rpm. The low n makes this waterwheel needs a high ratio transmission to be connected with the generator to harvest its mechanical energy to electrical energy [11,17]. The high transmission ratio makes the application of breastshot waterwheels more complicated, with additional losses which affect its performance [18,19]. The higher n could be attained by increasing the inlet tangential velocity and decreasing the D. The strategy of this study was to convert the potential energy into kinetic energy and to direct it into the buckets just above the waterwheel shaft. Hence, this study examines the feasibility of breastshot waterwheels with a small diameter and modifying the bucket inlet angle (β) to use the computational fluid dynamics (CFD) method in ultra-low-head conditions.

2. Methodology

2.1 Water Wheel Design and Modeling

This waterwheel has been designed to work on a dammed river that generates one meter of the potential head. The diameter and potential head ratio (D/H) of the breastshot waterwheel chosen is 1. 1 D/H is smaller than the recommendation in prior studies [16,20,21]. The hydraulic depth of the inflow (h_u) is 0.45 m to increase the water kinetic energy; theoretically, this condition could generate an inflow velocity (C_1) of about 3 m/s. The design parameters and the size are briefly shown in Table 1.

Table 1
Breastshot water wheel design parameters

Parameters	Dimension
Gross potential head (H)	1 m
Channel depth (h_c)	0.18 m
Inflow depth (h_u)	0.45 m
Outflow depth (h_t)	0.1 m
Wheel's diameter (D)	1 m
Wheel's bucket's depth (d_s)	0.2 m
Bucket's deep angle (β_D)	50°
Bucket's deep radius (R_2)	0.15 m
The angle of attack (α)	30°
Bucket's inlet angle (β)	36°, 49°, 71°, and 90°
Inflow width angle	5°
Inflow width (S_1)	0.1131 m
Channel width	0.5 m

Then, Figure 1-a shows the two-dimensional (2D) design of the waterwheel. Therefore, the strategy of this study was to convert the potential energy into kinetic energy and direct it into the buckets just above the water wheel shaft.

The wheel rotation for simulation setup of 15 to 45 rpm, this to know the optimum velocity ratio condition of this waterwheel. In previous discussions, Muller [8] found that the optimum U/C_1 was 0.6. However, Quaranta and Revelli [15] recommend the velocity ratio of this waterwheel as 0.4. In contrast, based on Euler's momentum theory, the optimum U/C_1 should be 0.5. The optimum of U/C_1 does not depend on the C_1 but also on the potential energy exchange, the blade inclination, and the bucket shape. Therefore, the bucket inlet angle (β) is important to vary, using the following angles of 36°, 49°, 71°, and 90°. This β was the suitable inlet angle for mentioned U/C_1 ratios based on velocity triangle approach. Figure 1-b shows the variation of β.

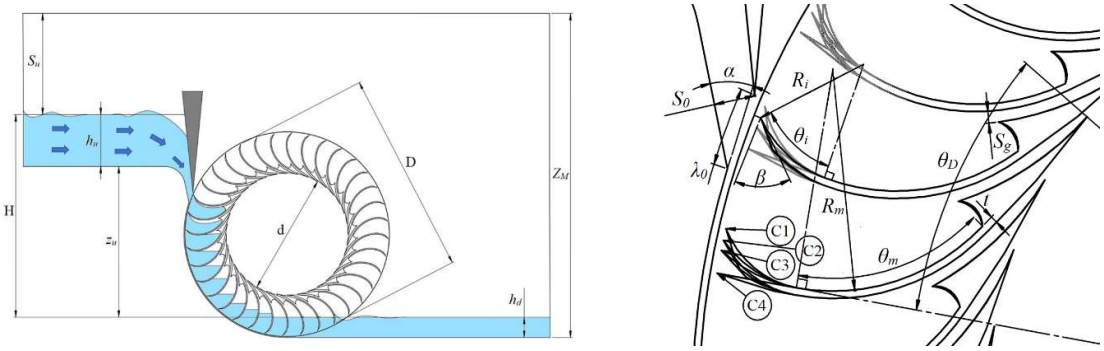

(a) (b)

Fig. 1. Case study geometry: (a) General design, and (b) Inflow and bucket configurations

The modeling of the breastshot waterwheel working process using the planar two-dimensional simulation. The pressure in the inlet is set as a boundary condition (BC) at 1,765 Pa to keep the potential head stable due to the possibility of fluctuating water flow. The pressure outlet has been used to keep the wheel immersion depth condition. The surrounding boundary also used a pressure outlet at atmospheric pressure. Figure 2 shows the boundary condition.

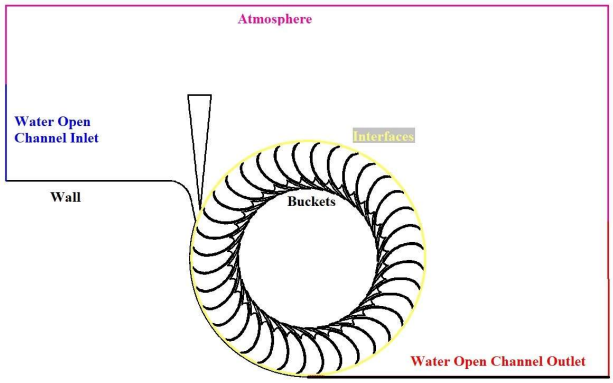

Fig. 2. Boundary condition

2.2 Meshing and Time Discretization

The breastshot waterwheel model was divided into about 63,000 elements of the numerical mesh. The 63,000 mesh elements were obtained from the mesh independency process using the Richardson extrapolation method. They were tested in three meshing sizes, which are 1 mm (254k mesh), 2 mm (63k mesh), and 4 mm (16k mesh). The Richardson extrapolation method is called the grid convergency index (GCI) [21]. Based on GCI analysis, the error of 254k elements was about 0.01%, the 63k elements mesh of 0.17%, and the 16k elements mesh of 4.53%. Thus, the simulation used 63k elements of the mesh. Furthermore, the y^+ number was kept between 30 to 300 with the mesh adaption feature. The visualization of 63k mesh is presented in Figure 3. Then, the simulation timestep was 0.002 s [1,15,23], where the error of 1% to 3%.

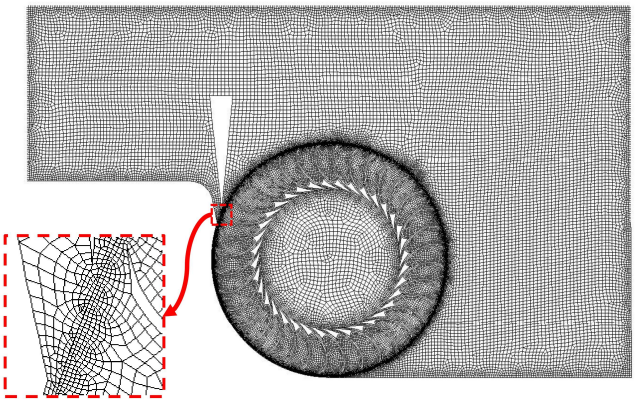

Fig. 3. Visualization of mesh

2.3 Simulation Specification

The simulation ran using ANSYS® Fluent 19.1™ Academic Version with a feature moving mesh dynamic approach. The moving mesh rather than six degrees of freedom (6-DOF) to avoid charging phenomena bias; the phenomena have been reported in previous studies [22]. The pressure-based approach of mass conservation; the governing equation for the mass conservation for pressure based on the transient condition of:

$$\frac{\partial(\rho)}{\partial t}+\frac{\partial(\rho u_j)}{\partial x_j}=0 \tag{1}$$

It is assumed the fluid flow is turbulent. Therefore, the governing equation Reynolds Average Navier-Stokes is applied as a numerical calculation of fluid flow momentum:

$$\frac{\partial(\rho u_i)}{\partial t}+\frac{\partial(\rho u_i u_j)}{\partial x_j}=-\frac{\partial p}{\partial x_i}+\frac{\partial(\tau_{ij}-\rho u_i{'}u_j{'})}{\partial x_j}+\rho g_i \tag{2}$$

p is pressure, τ_{ij} is shear stress, and $-\rho u_i{'}u_j{'}$ is Reynolds stress. The numerical calculation for the $-\rho u_i{'}u_j{'}$ is [23]:

$$-\rho u_i{'}u_j{'}=\mu_t\left(\frac{\partial u_i}{\partial x_j}+\frac{\partial u_j}{\partial x_i}\right)-\frac{2}{3}\left(\rho k+\mu_t\frac{\partial u_i}{\partial x_i}\right)\delta_{ij} \tag{3}$$

Then, the standard k-ε is the turbulence model for numerical calculation for the physical phenomenon of turbulence flow. The governing equation for the standard k-ε is [25,26], for *k*:

$$\frac{\partial(\rho k)}{\partial t}+\frac{\partial(\rho k u_i)}{\partial x_j}=\frac{\partial}{\partial x_i}\left(\left(\mu+\frac{\mu_t}{\sigma_k}\right)\frac{\partial k}{\partial x_j}\right)+G_k+G_b+\rho\varepsilon+Y_M+S_k \tag{4}$$

and for ε [24]:

$$\frac{\partial(\rho\varepsilon)}{\partial t}+\frac{\partial(\rho\varepsilon u_i)}{\partial x_j}=\frac{\partial}{\partial x_i}\left(\left(\mu+\frac{\mu_t}{\sigma_\varepsilon}\right)\frac{\partial\varepsilon}{\partial x_j}\right)+C_{1\varepsilon}\frac{\varepsilon}{k}(G_k+C_{3\varepsilon}G_b)-C_{2\varepsilon}\rho\frac{\varepsilon^2}{k}+S_\varepsilon \tag{5}$$

The breastshot waterwheel operates at atmospheric pressure, so the volume of fluid (VoF) approach is necessary for the simulation. The governing equation for VoF is, for density (ρ):

$$\rho=\alpha_w\rho_w+\alpha_a\rho_a \tag{6}$$

and for viscosity (μ):

$$\mu=\alpha_w\mu_w+\alpha_a\mu_a \tag{7}$$

Then, the surface tension modeling between water and air was set at 0.0728 N/m. The simulation was run with pressure at the inlet, which was specified as 1,765 Pa, and the inlet channel depth was 0.18 m. The pressure at the water outflow pressure outlet was 981 Pa; the immersion depth was 0.1 m. The simulation used two zones, the rotating and the static zone, that have connected each other with an interface. The wall BC of the bucket was specified as a moving wall, which is considered rotating at a certain angular velocity, by the moving mesh option.

The SIMPLE pressure-velocity coupling scheme to solve the governing equations was used. Cell-based least square gradient method and first-order upwind method momentum, turbulent kinetic

energy, and turbulent dissipation rate spatial-based discretization were used for the solution solving. The PRESTO method was used to discretize the pressure. The initialization was referred to the surrounding outlet, with an air volume fraction equal to one. Furthermore, the inflow channel region was marked to be patched with zero air volume fraction. Furthermore, the simulation was run for 1400 timesteps, with the maximum number of iterations per timestep being 150.

3. Results and Discussions

3.1 Transient Simulation Process

The simulation ran for 4000 timesteps resulting in 4 seconds of simulation time. Data generated from the simulation were saved automatically every two timesteps; data is processed when the mass and torque flows stabilize. The transient process from the beginning of the simulation to the steady condition of β of 36° and 40 rpm case is briefly displayed in Figure 4.

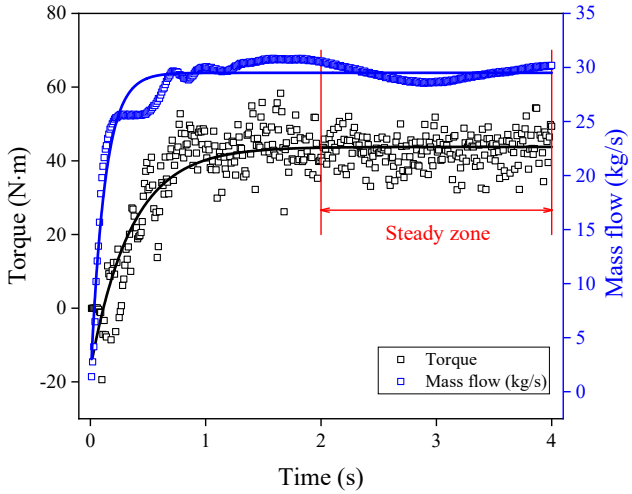

Fig. 4. The simulation results - the transient process

3.2 Simulation Results

Figure 5 shows the relation of τ and P_m to n; a for τ and P_m to n expressed by linear, and b for P_m to n is parabolic. From the linear approach (Figure 5-a), the 71° bucket generates a torque of 85.3 N·m higher than the 49° of 78.38 N·m, 36° of 73.11 N·m, and 90° 49.52 N·m. From the parabolic approach (Figure 5-b), P_m maximum for bucket 36° and 90° occurs at 35 rpm, and for 49° and 71° occurs at 30 rpm. Based on Figure 5-b, the bucket 71° generates P_m of 171.9 W higher than the 36° of 165.21 W, the 49° of 165.11 W, and 90° of 128.84 W.

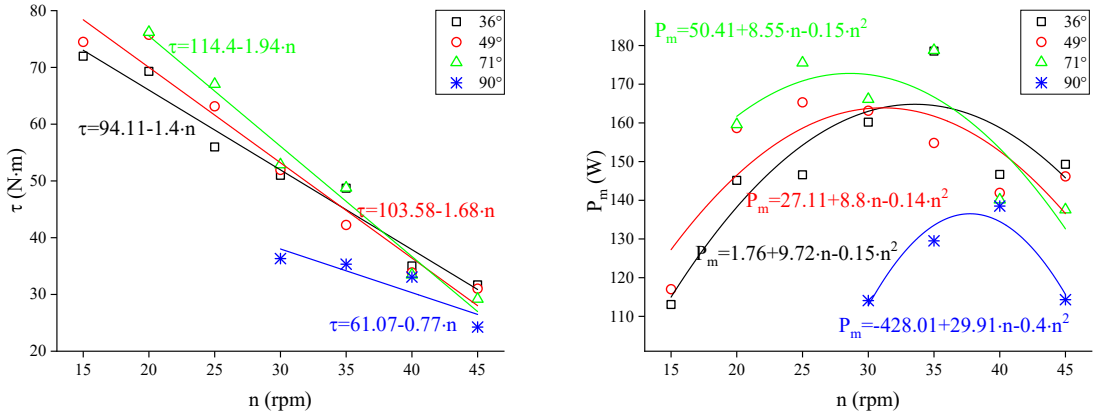

(a) (b)

Fig. 5. Simulation results: (a) Relation of τ to n; and (b) Relation of P_m to n

Figure 6 shows the relation of performance (η) to n expressed by parabolic. Based on the parabolic approach, the η maximum of 36° bucket of 79.96% is higher than 71° of 74.94%, 49° of 66.3%, and 90° of 58.7%. The 36° bucket has an unfavourable hydraulic behaviour (significant decreases in performance) when wheel rotation changes. From Figure 6, the 71° bucket performs better than 36° and 90°. However, from operating condition (n), the 49° bucket more preferable because the wheel rotation changes performance decrease is not significant.

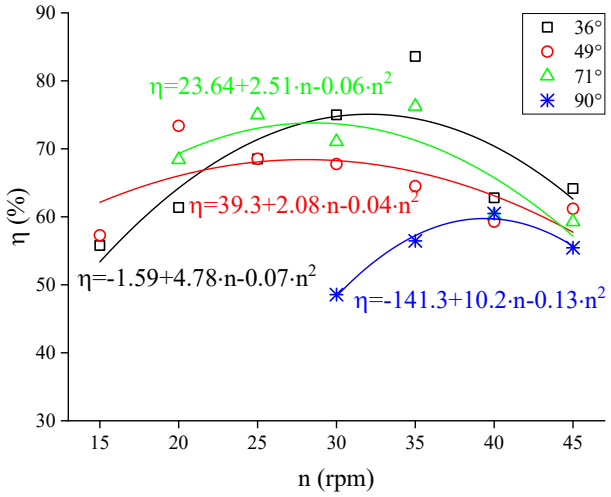

Fig. 6. Relation of η to n

3.3 Discussion

Quaranta and Revelli [15] recommend the U/C_1 0.4 for optimum breastshot waterwheel performance. The U/C_1 ratio for the breastshot waterwheel is ambiguous. Water entering the blade is relatively calm ($C_1 \rightarrow 0$ m/s) and has potential energy (head); this condition is similar to Archimedes turbine. For the breastshot waterwheel, operating conditions are more relevant to use a specific speed (N_s); calculation of N_s using:

$$N_s = \frac{n \cdot (\rho \cdot g \cdot Q \cdot H)^{0.5}}{\rho^{0.5} \cdot (g \cdot H)^{1.25}} \quad (8)$$

Figure 7 shows the relation of η to n, expressed by parabolic. Based on Figure 7, a 49° bucket is recommended for use since it has a stable efficiency above 60% with a range of N_s from 0.4 to 1.2. The N_s range of a 49° bucket is similar to the parabola fit range of all data. The proposed 49° bucket breastshot waterwheel has better performance than the previous research [15,23]. The wide N_s range defines that large discharge fluctuations do not change the turbine performance significantly; this is to be expected on the site.

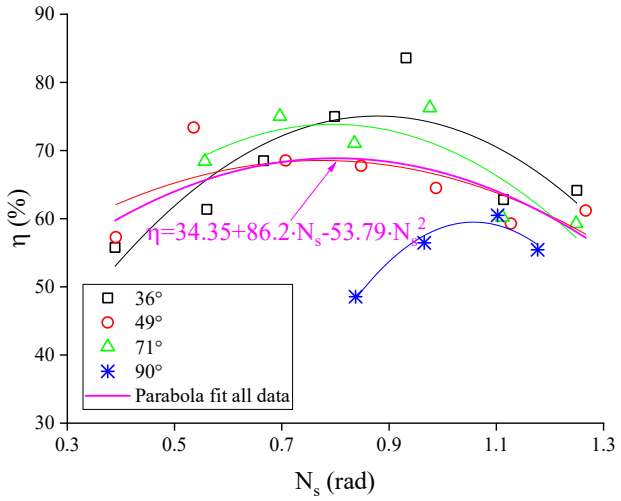

Fig. 7. Relation of η to N_s

The determination of the influence of β and n (variable) to η (response) for data in Figure 6 is using the response surface method (RSM). The significance of the effect of β and n on η depicted using Eq. (9). The accuracy Eq. (9) by root means square error (RMSE) of 9.02%; categorized is verified.

$$\eta = j_1 + j_2 \cdot \beta + j_3 \cdot n + j_4 \cdot \beta^2 + j_5 \cdot n^2 + j_6 \cdot n \cdot \beta \quad (9)$$

Where [j_1, j_2, j_3, j_4, j_5, j_6] of [19.62, 0.18, 3.46, -0.012, -0.075, 0.03]. Then, based on Table 2, F more than $F_{significance}$ means β and n significantly affect η (response).

Table 2
Analysis of variance relation of β and n to η

	Degree of freedom	Sum of square	Mean square	F	$F_{significance}$
Regression	5	3644.28	728.86	6.71	0.0011
Residual	18	1954.06	108.56		
Total	23	5598.35			

Figure 8 shows the fraction of water within the control volume. From Figure 8, the 71° bucket generates greater torque than others, presumably because no water downstream is trapped in the bucket, so it does not block wheel rotation. The graph where the behaviour of the torque is shown in Figure 5-a. For 36° and 49° in Figure 8, water before going downstream looks stuck at the end of the bucket arm; this condition is not preferred in waterwheels because it becomes lost. In the case of a 90° bucket, the water contained in all active blades looks proportional, which is advantageous.

Based on Figure 5-a, the torque generated by the 90° bucket is not as expected; presumably, the water flowing into the next active blade through the leakage between the wheel and the channel wall is a rotational flow. Rotational flow is indicated by an air phase formed in the middle of the water phase; it looks like a lot of water in a 90° bucket on its active blade. Therefore, based on the phenomenon of water volume fraction in Figure 8, the reasonable 71° bucket converts water energy into torque better than the others; still, a bucket with higher torque is not necessarily recommended.

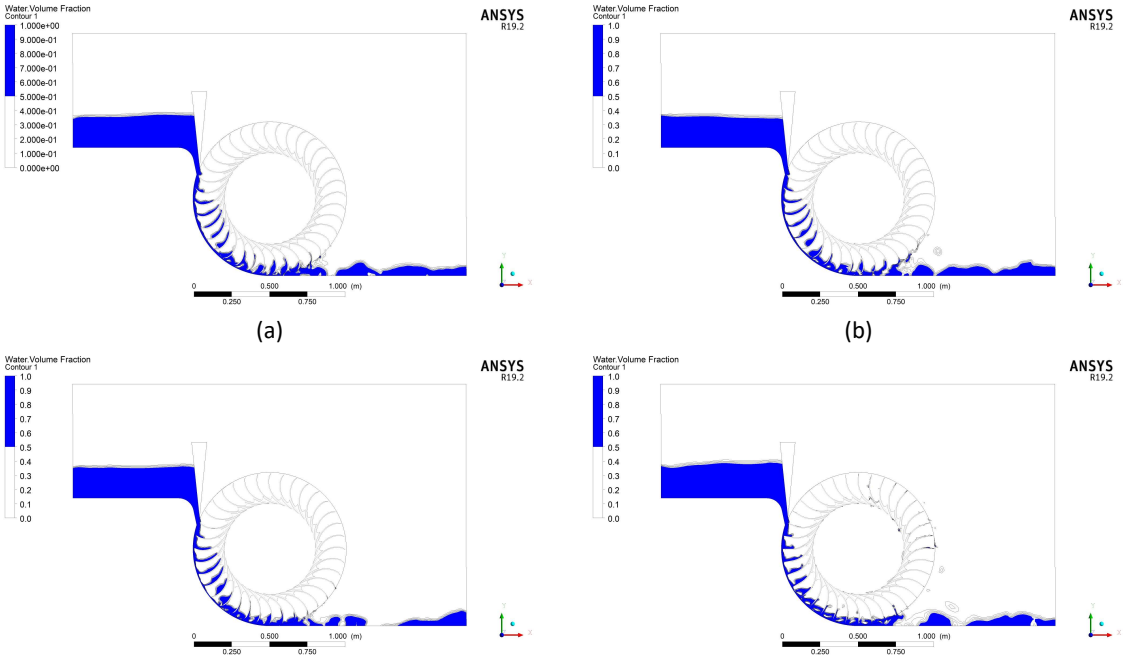

Fig. 8. Visualization of water volume fraction: (a) 36°; (b) 49°; (c) 71°; and (d) 90°

Figure 9 shows the velocity contour. Figure 9 is similar to Figure 5 and Figure 8, where the torque generates by the 71° bucket is greater since the water volume it holds is more than the others. Then, for the 71° bucket, the active bucket at the top hold, and the water has velocity. The positive effect of water on the velocity in the bucket is wheel rotation increases, and the natural consequence effect is the wheel vibration generated certainly increases (negative effect). The vibrations in the turbine are avoided because they can damage civil construction and cause mechanical joining wear. For the 36° bucket and 90° bucket, a lot of water downstream still has velocity; this indicates the water potential energy is not maximally converted. In contrast, for a 49° bucket, the water velocity in the downstream ranges by 0.3 to 0.5 m/s, indicating the water potential energy is properly converted into mechanical energy. Therefore, based on Figure 7 and Figure 9, the recommended breastshot waterwheel bucket inlet angle for this case is 49°.

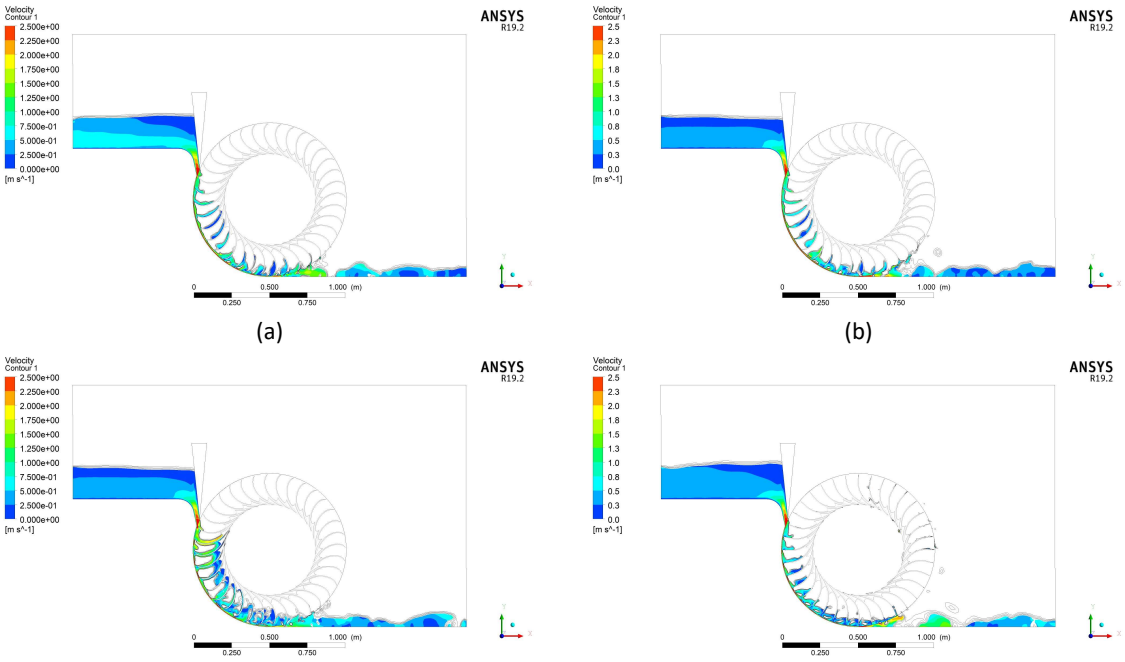

Fig. 9. Visualization of velocity contour: (a) 36°; (b) 49°; (c) 71°; and (d) 90°

Furthermore, the performance was good enough for simple electricity harvesting in isolated rural areas with perennial stream rivers. This study reveals that the breastshot water wheel can work well at 35 rpm (rotational speed), which means that this water wheel only needs of 1:50 transmission to be coupled with an alternating current (AC) generator. This is simpler than using three or more stages of 1:100 – 1:200 transmission. The increase of simplicity of this water wheel is believed to make the breastshot water wheel more reliable in generating electricity, especially in isolated rural areas in Indonesia.

4. Conclusions

The breastshot waterwheels have good simplicity, efficiency, and low-head range [3,4] since they are suitable to be used in a tropical rainforest village in Indonesia [5]. The weakness of the breastshot waterwheel is it's very slow rotational speed (n) between 7.5 to 20 rpm [15]. Reasonably, the higher n could be attained by increasing the inlet tangential velocity and decreasing the wheel diameter (D). The strategy of this study was to convert the potential energy into kinetic energy and direct it into the buckets just above the waterwheel shaft. Hence, this study examines the feasibility of breastshot waterwheels with a small diameter and modifying the bucket inlet angle (β) to use the computational fluid dynamics (CFD) method in ultra-low-head conditions. The D/H ratio for CFD method of 1 with four vary β (36°, 49°, 71°, and 90°). The D/H ratio of is smaller than recommendation [9] of twice of the H (head). Based computational results, the β and n affect the performance of breastshot waterwheel and expressed using parabolic. The performance maximum for 36° bucket of 79.96% is higher than 71° of 74.94%, 49° of 66.3%, and 90° of 58.7%. Based on specific speed (N_s) considerations, 49° bucket more preferable because as a stable efficiency above 60% with a range of N_s from 0.4 to 1.2. The wide N_s range defines that large discharge fluctuations do not change the turbine performance significantly; this is to be expected on the site.

Acknowledgement
The research/publication of this article was funded by DIPA of Public Service Agency of Universitas Sriwijaya 2023. SP-DIPA-023.17.2.677515/2023, on November 13, 2022. In accordance Rector's Decree Number: 0189/UN9.3.1/SK/2023, on April 18, 2023.

References

[1] Pps, Jonathan Sahat, Dendy Adanta, and Aji Putro Prakoso. "Influence of bucket shape and kinetic energy on breastshot waterwheel performance." In *2018 4th international conference on science and technology (ICST)*, pp. 1-6. IEEE, 2018.
[2] Müller, Gerald, and Klemens Kauppert. "Old watermills—Britain's new source of energy?." In *Proceedings of the Institution of Civil Engineers-Civil Engineering*, vol. 150, no. 4, pp. 178-186. Thomas Telford Ltd, 2002. https://doi.org/10.1680/cien.2002.150.4.178
[3] Syafriyudin, Fajar B., S. H. Winoto, and M. Facta. "Early analysis of jumping water effect on breastshot waterwheel for microhydro power plant." In *J Phys Conf Ser*, vol. 953, p. 12039. 2018. https://doi.org/10.1088/1742-6596/953/1/012039
[4] Müller, Gerald, and Klemens Kauppert. "Performance characteristics of water wheels." *Journal of Hydraulic Research* 42, no. 5 (2004): 451-460. https://doi.org/10.1080/00221686.2004.9641215
[5] Adanta, Dendy, Budiarso Budiarso, Warjito Warjito, Ahmad Indra Siswantara, and Aji Putro Prakoso. "Performance comparison of NACA 6509 and 6712 on pico hydro type cross-flow turbine by numerical method." *Journal of Advanced Research in Fluid Mechanics and Thermal Sciences* 45, no. 1 (2018): 116-127.
[6] Helmizar, Helmizar. "Turbine wheel-a hydropower converter for head differences between 2.5 and 5 m." PhD diss., University of Southampton, 2016.
[7] Breeze, Paul. *Hydropower*. Academic Press, 2018. https://doi.org/10.1016/B978-0-12-812906-7.00006-5
[8] Müller, G., and Christian Wolter. "The breastshot waterwheel: design and model tests." In *Proceedings of the Institution of Civil Engineers-Engineering Sustainability*, vol. 157, no. 4, pp. 203-211. Thomas Telford Ltd, 2004. https://doi.org/10.1680/ensu.2004.157.4.203
[9] Bach, Carl. *Die Wasserräder*. BoD–Books on Demand, 2013.
[10] Quaranta, Emanuele, and Roberto Revelli. "Performance characteristics, power losses and mechanical power estimation for a breastshot water wheel." *Energy* 87 (2015): 315-325. https://doi.org/10.1016/j.energy.2015.04.079
[11] Quaranta, E., and R. Revelli. "Optimization of breastshot water wheels performance using different inflow configurations." *Renewable Energy* 97 (2016): 243-251. https://doi.org/10.1016/j.renene.2016.05.078
[12] Quaranta, Emanuele, and Roberto Revelli. "Hydraulic behavior and performance of breastshot water wheels for different numbers of blades." *Journal of Hydraulic Engineering* 143, no. 1 (2017): 04016072. https://doi.org/10.1061/(ASCE)HY.1943-7900.0001229
[13] Adanta, Dendy, and Aji P. Prakoso. "The effect of bucketnumber on breastshot waterwheel performance." In *IOP Conference Series: Earth and Environmental Science*, vol. 105, no. 1, p. 012031. IOP Publishing, 2018. https://doi.org/10.1088/1755-1315/105/1/012031
[14] Adanta, Dendy. "The effect of channel slope angle on breastshot waterwheel turbine performance by numerical method." *Energy Reports* 6 (2020): 606-610. https://doi.org/10.1016/j.egyr.2019.11.126
[15] Quaranta, Emanuele, and Roberto Revelli. "Gravity water wheels as a micro hydropower energy source: A review based on historic data, design methods, efficiencies and modern optimizations." *Renewable and Sustainable Energy Reviews* 97 (2018): 414-427. https://doi.org/10.1016/j.rser.2018.08.033
[16] Williamson, Sam J., Bernard H. Stark, and Julian D. Booker. "Low head pico hydro turbine selection using a multi-criteria analysis." *Renewable Energy* 61 (2014): 43-50. https://doi.org/10.1016/j.renene.2012.06.020
[17] Michaelis, Klaus, Bernd-Robert Höhn, and Michael Hinterstoißer. "Influence factors on gearbox power loss." *Industrial lubrication and tribology* 63, no. 1 (2011): 46-55. https://doi.org/10.1108/00368791111101830
[18] Nelias, D., P. Sainsot, and L. Flamand. "Power loss of gearbox ball bearing under axial and radial loads©." *Tribology transactions* 37, no. 1 (1994): 83-90. https://doi.org/10.1080/10402009408983269
[19] Chaudy, F. "Machines hydrauliques, Bibliothèque du conducteur de travaux publics." *Vve. C. Dunod et P. Vicq* (1896).
[20] Busquet, Raymond. *A manual of hydraulics*. E. Arnold, 1906.
[21] Adanta, Dendy, Mochammad Malik Ibrahim, Dewi Puspita Sari, Imam Syofii, and Muhammad Amsal Ade Saputra. "Application of the Grid Convergency Index Method and Courant Number Analysis for Propeller Turbine

Simulation." *Journal of Advanced Research in Fluid Mechanics and Thermal Sciences* 96, no. 2 (2022): 33-41. https://doi.org/10.37934/arfmts.96.2.3341

[22] Prakoso, Aji Putro, Dendy Adanta, and Ridho Irwansyah. "Approach for a breastshot waterwheel numerical simulation methodology using six degrees of freedom." *Energy Reports* 6 (2020): 611-616. https://doi.org/10.1016/j.egyr.2019.11.127

[23] Hakim, Muhammad Luqman, Bagus Nugroho, Rey Cheng Chin, Teguh Putranto, I. Ketut Suastika, and I. Ketut Aria Pria Utama. "Drag penalty causing from the roughness of recently cleaned and painted ship hull using RANS CFD." *CFD Letters* 12, no. 3 (2020): 78-88. https://doi.org/10.37934/cfdl.12.3.7888

[24] Fluent, A. N. S. Y. S. "Release 15.0, theory guide." *ANSYS Inc, Canonsburg* (2013).

[25] Alfarawi, Suliman SS, Azeldin El-sawi, and Hossin Omar. "Exploring discontinuous meshing for cfd modelling of counter flow heat exchanger." *Journal of Advanced Research in Numerical Heat Transfer* 5, no. 1 (2021): 26-34.

[26] Budiarso, Budiarso, Helmizar Helmizar, Warjito Warjito, Agus Nuramal, Wahyu Ramadhanu, and Dendy Adanta. "Performance of breastshot waterwheel in run of river conditions." In *AIP Conference Proceedings*, vol. 2227, no. 1. AIP Publishing, 2020. https://doi.org/10.1063/5.0000940